Frequency Locked Loop-Based Control Algorithm with Enhanced Second-Order Generalized Integrator for PV-Battery Integrated System to Improve Power Quality

Nirmal Kumar Pandey*, Rupendra Kumar Pachauri *, Sushabhan Choudhary*, Sudhakar Babu Thanikanti**

*Electrical Cluster, School of Engineering, University of Petroleum and Energy Studies, Dehradun, 248007, India

**Electrical Engineering Department, Chaitanya Bharathi Institute of Technology, Telangana, 500075, India.

(nirmalpande84@gmail.com, rpachauri@ddn.upes.ac.in, schoudhury@ddn.upes.ac.in, sudhakarbabu66@gmail.com)

‡Corresponding Author; Nirmal Kumar Pandey, University of Petroleum and Energy Studies, Tel: +91 8109167303, nirmalpande84@gmail.com

Received: 22.05.2023 Accepted:14.07.2023

Abstract- This study proposes a control approach based on a frequency-locked loop with an Enhanced Second-Order Generalized Integrator (ESOGI-FLL) to mitigate power quality (PQ) problems in a grid-linked photovoltaic (PV) battery scheme. In order to enhance PV power production, charge the battery, pump it into the grid, and maintain the constant voltage across the DC bus of the voltage source inverter, particle-swam optimized Adaptive Neuro Fuzzy Inference System (PSO-ANFIS)-controlled peak power point extracting methods are employed in this study. This paper utilizes the ESOGI-FLL-based control technique to achieve grid current balancing, mitigate harmonics, operate at unity power factor, and accommodate various levels of PV energy generation. Frequency Locked Loop with Enhanced Second Order Generalized Integrator with Based Regulator Algorithm for PV Battery Integrated System for PQ Improvement is created and tested in MATLAB software. Simulation results are tested under various operating situations, such as grid current balancing, Nonlinear load conditions, and changing irradiance conditions. Additionally, grid and currents have total harmonic distortions of 0.95% and 2.03% for unbalanced load changes in irradiance conditions, and these are under the IEEE power quality standard.

Keywords- ANFIS, Battery system, ESOGI-FLL, MPPT, PSO, PV system, Power quality

1. Introduction

According to sources [1, 2], the majority of electricity production in India, which accounts for 68% of total power generation, is reliant on non-renewable fossil fuels such as coal and oil. This conventional method of power generation through fossil fuels contributes to the emission of greenhouse gases, resulting in environmental impacts [2]. Energy security faces significant challenges due to high peak power demand, reliance on imports for oil and, to a growing extent, coal, and inadequate energy supply. These factors collectively contribute to major concerns regarding energy security. Energy consumption and output have to be in equilibrium. In order to slow down the effects of climate change, household power production must be started in the distribution system utilizing standalone Photovoltaic (PV) arrays. As a result, small-scale applications for rooftop PV arrays are rapidly expanding [3]. But PV power is available only during the daytime, and we are not able to use it at night. This can be overcome by combining PV power generation with battery storage elements and connecting to the grid system. Quality of power issues in the delivery network primarily stem from loads with nonlinear properties, which include motor drives, variable speed drives, arc furnaces, UPSs, residential loads, and other equipment that consumes imaginary power at the connecting point of PV inverters. These nonlinear loads have a negative impact on the power quality of the grid. In [4], GMPP tracking for a grid-connected PV system under partial shade conditions has been presented using a hybrid artificial neural network utilizing deep reinforcement learning. The Voltage Source Converter (VSC), which links PV and batteries to the grid, may be set up in a number of different ways, as suggested in [5]. The literature [6] demonstrates the loss examination for two phase and single stage PV power generation schemes (PGSs). Compared to double stage-PGS, single-stage PGS

offers certain benefits, including greater efficiency, less complexity, and fewer components (capacitor, diode, etc.).

The quality of power on the grid is often diminished owing to the presence of loads with nonlinear properties such as arc furnaces, computers, heavy rectifiers, lamps, printers, UPSs, and adjustable frequency motors, which are usually linked at the common point of coupling [6]. The difficulties in employing renewable energy sources to improve the quality of power in the system are discussed in [7]. A multi-functional method based on the ABC-DQ transformation has been presented by Javadi et al. [8] for noise reduction, balancing the load, compensating reactive power, and zero voltage control. The transformation-based control approach shows inadequate dynamic performance across different operating scenarios, characterized by second harmonic oscillations in the direct axis current caused by an unbalanced load network. To address power quality concerns in distribution grids, a control algorithm known as Least Mean Fourth (LMF) [9] has been proposed. This algorithm facilitates phase-independent modulation of the basic load current amplitude. The LMF algorithm's stable state convergence degree is suboptimal, likely owing to its quarter-order optimization. To enhance the quality and power of a single-phase scheme, a Model Predictive Control (MPC) strategy has been introduced [10]. However, the MPC approach is associated with high computational and memory requirements. A notch filter-based approach is investigated for incorporating distributed generation into the network. The Phase Locked Loop (PLL)-less method [11] is less effective at mitigating DC components and harmonics, and system performance deteriorates when DC offset components are present in the load currents. In [12], a sliding mode-based technique with a Lyapunov function is proposed to improve the quality of power in the distribution grid. However, the converter experiences aggressive switching due to the sliding mode control, leading to a shorter lifespan. In [13], a Kalman filter-based approach is introduced for PV-linked grid energy conversion schemes. The Kalman filter approach is sophisticated, requires more memory, and has a high computational overhead. Under different system parameters, the Kalman filter's parameter adjustment is challenging and extremely sensitive. To isolate the basic load component, the Least Square (LS) built-in regulator approach is proposed [14]. However, when the system frequency varies, the LS algorithm's accuracy is in question.

In the literature, utility interactive inverters are discussed in [15] for improving power quality with the application of a five-level shunt active filter and sliding mode control. [16-17] presents a comprehensive control strategy for the distribution network's shunt active power filter. The characteristics for balancing grid currents are absent from this control algorithm. The dynamic performance algorithms based on neural networks [18] are subpar when the load-side network is unbalanced. Due to the individual layer neural network method's subpar magnitude extraction capabilities, PPGS performance is compromised. A large number of datasets are required for the training of the neural network method. As a result of the system's inability to completely remove the load current DC offset component. To enhance power quality in the distribution grid, adaptive filter-based regulator methods are presented in the existing work. These approaches include the Least Mean Square (LMS) technique [19] and the least logarithmic absolute difference method [20]. The LMS procedure exhibits a lower convergence rate than the LMF method. Additionally, the LMS procedure results in a more squared mean error when approximating the amplitude of the basic current of the load. The back circulation approach is quite sophisticated when it comes to layer design and data training. In weak grid scenarios and when DC offset is present in load current, the efficacy of adaptive filter-based regulator approaches [9–20] is a matter of debate. To address the system's stability in such situations, the literature proposes a solution in [21].

Various generalized integrators have been proposed for PV battery-linked grid systems, including the SOGI and Second Order Generalized Integrator-Quadrature (SOGI-Q) methods. These techniques are detailed in [22–25]. When more harmonics, frequency variations, and DC offset variations are present, the SOGI-Q and SOGI algorithms perform poorly in terms of system performance. The main contribution of the work is the ESOGI-FLL-based control scheme, which offers enhanced abilities to sift DC offset and reject harmonics. This approach is particularly reliable for estimating the quadrature component of fundamental load current, providing more accurate results than other techniques.

When compared to traditional control logic techniques, the ESOGI-FLL-based regulator provides improved steady-state and dynamic responsiveness, along with strong DC component and harmonic reduction capabilities. The feed-forward component is supported by the suggested ESOGI-FLL-based control approach, which reduces variations in the grid currents caused by divergence in PV power generation and loads [26–29]. The PSO-ANFIS procedure is employed in the voltage source inverter controlling approach to produce the voltage bus DC reference for extracting peak power from array PV panels and to improve pumping of PV power to the macro network. The ESOGI-FLL algorithm offers superior performance in both stable state and dynamic circumstances, with greater precision, lower fluctuations in magnitude approximation, and lower difficulty and computational requirements than traditional algorithms.

MATLAB/Simulink is used to simulate outcomes for a variety of operational situations, including network load unbalance and solar radiation fluctuation, to validate the efficiency of the control algorithm.

2. PV Battery Integrated Grid System and Its Control

Fig. 1 depicts the PV Battery integrated grid system, which consists of a ripple filter, a voltage source converter, interface inductors, a PV grid with a three-phase scheme, Battery energy storage, and Non-Linear and Unbalanced loads. The voltage source inverter switching ripple produces higher-order harmonics, which are reduced by the ripple filter. To lessen current harmonics in PV battery-linked voltage source converters, an interface inductor is utilised.

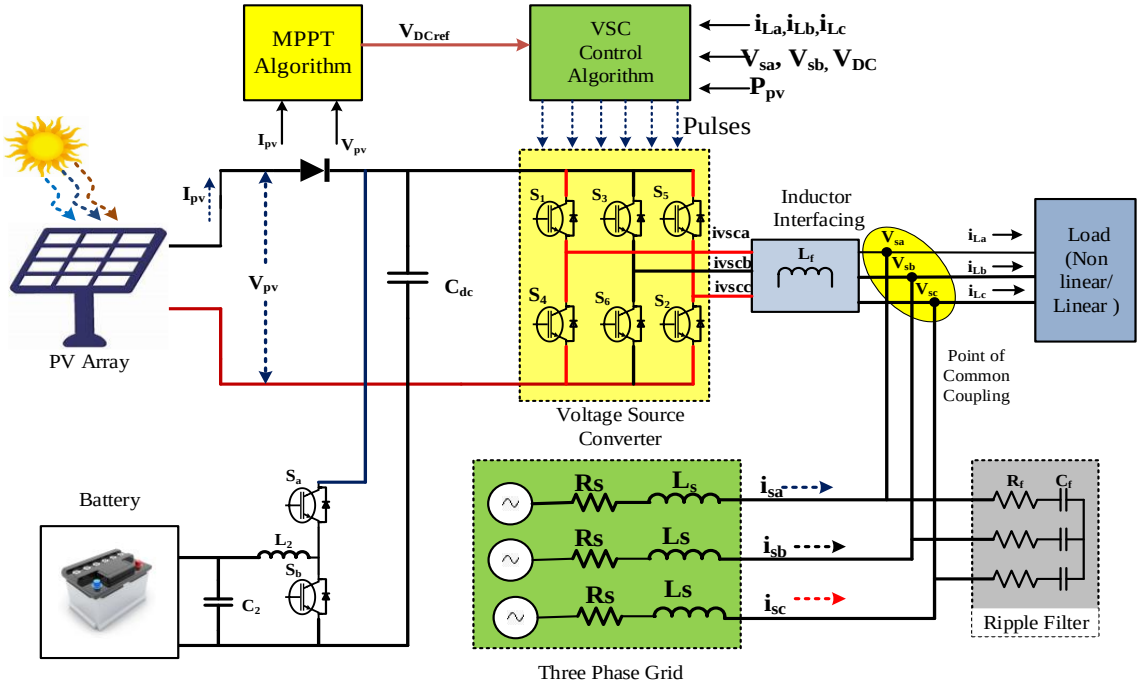

Fig.1. PV battery Integrated Grid system

The layout of the ESOGI-FLL-based control method is demonstrated in Fig. 2, which consists of several components. The array of PV panels is operated using the PSO-ANFIS-based peak power extractor algorithm to maximize power production. The ESOGI-FLL method is employed to extract the quadrature component of the vital current of the load. The regulator procedure comprises PSO-ANFIS techniques and control of the switching of the voltage source converter. The PSO-ANFIS techniques are utilized to produce the DC link reference voltage.

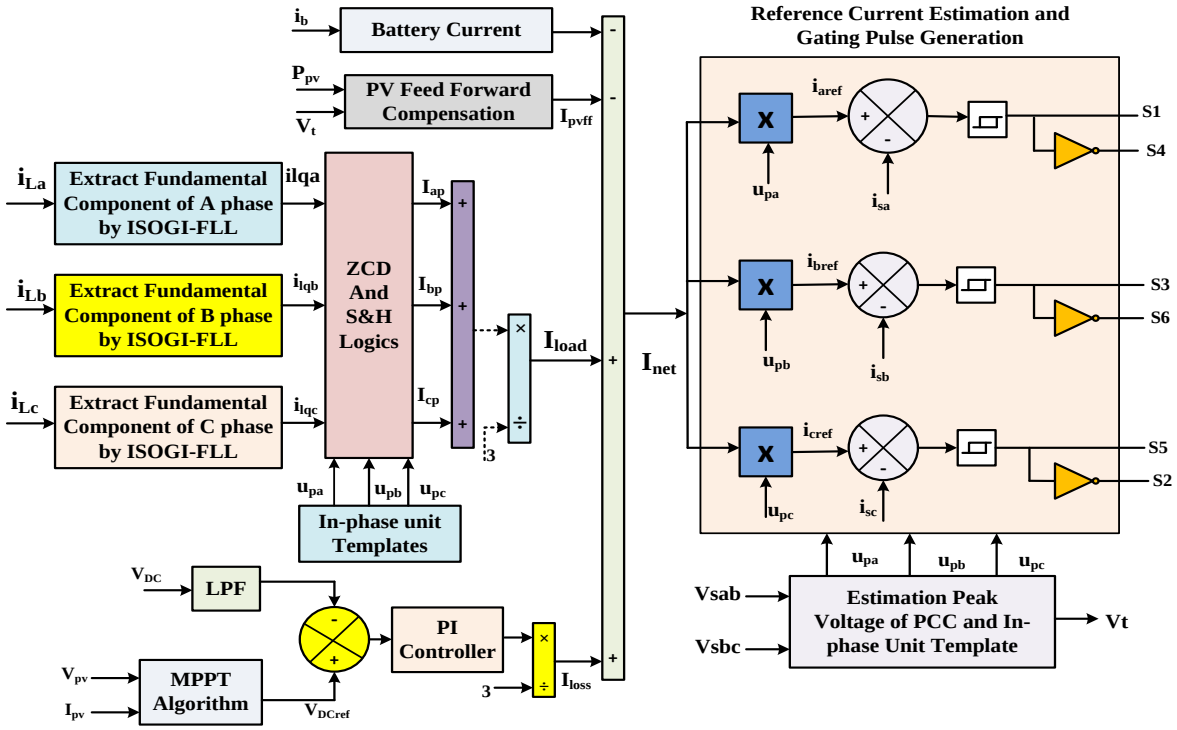

Fig.2. Control Logic of PV battery Integrated Grid system

2.1 PSO-ANFIS Control for Maximum Power Extraction

The Maximum Power Point (MPP) is found using the PSO-ANFIS method. The PSO was used to tune the parameters of the ANFIS based on input and target data given to the ANFIS scheme. The Irradiance

and temperature details of the PV act as input information to the ANFIS system, and PV voltage at maximum power point conditions act as output information to the ANFIS system. The ANFIS input and output membership function values and rules between input and output are tuned using the PSO algorithm. After training using PSO, the ANFIS Network was used to obtain the maximum energy from PV and Provide position voltage for the DC bus voltage regulator. Fig. 3 shows the peak power extraction concept using PSO-ANFIS MPPT.

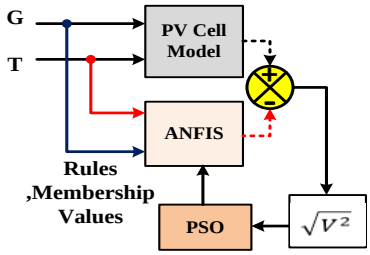

Fig.3. PSO-ANFIS control algorithm for Peak Power extraction

2.2 Control Current of the Battery Storage System

The Battery current is controlled by the PI control method. The power difference between PV and reference power for the grid is divided by battery voltage to generate reference current for the battery. The actual current for the battery is compared with the reference current of the battery and processed via the PI controller, and the PI controller generates the control signal for the PWM generator. The PWM generator generates the control pulse for the bidirectional converter to charge or discharge the battery based on the reference current. The control logic of the battery is shown in Fig. 4.

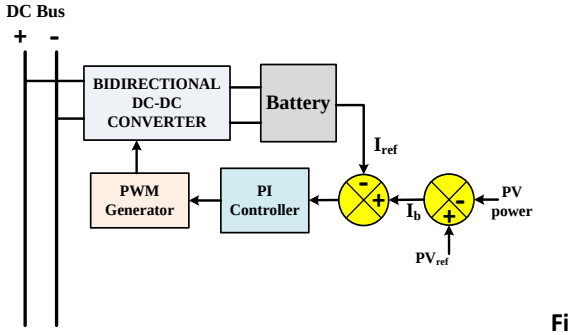

Fi

g.4. Control logic of the Battery storage system

2.3 Harmonic Mitigation Control Logic Using ESOGI-FLL for Voltage Source Converter

The estimates of PCC voltage amplitude, estimation of unit template Vector estimation, Feed Forward and Loss elements of PV systems, load fundamental current magnitude estimation, and estimation of grid current reference are all included in the control logic algorithm.

2.3.1 Unit Templates Vector Estimation

Phase voltage (Vsa,Vsb, Vsc) are determined based on the measured two-phase voltages (Vsab and Vsbc). In order to eliminate distortions, the Vsa and Vsbc signals are passed through a band-pass filter.

$$\begin{bmatrix} V_{sa} \\ V_{sb} \\ V_{sc} \end{bmatrix} = \frac{1}{3}\begin{bmatrix} 2 & 1 & 0 \\ -1 & 1 & 0 \\ -1 & -2 & 0 \end{bmatrix}\begin{bmatrix} V_{sab} \\ V_{sbc} \\ 0 \end{bmatrix} \quad (1)$$

The usual PCC voltage (V_t) is calculated as follows:

$$V_t = \sqrt{\frac{2}{3}(V_{sa}{}^2 + V_{sb}{}^2 + V_{sc}{}^2} \quad (2)$$

In order to estimate in-phase templates, phase voltages are divided by the terminal voltage's (V_t) amplitude, accordingly. The predicted values of these in-phase unit templates are

$$u_{pa} = v_{sa} / v_t, u_{pb} = v_{sb} / v_t, u_{pc} = v_{sc} / v_t \quad (3)$$

2.3.3 Feed Forward and Loss Element of PV System

The control method incorporates a PV feed-forward unit, which adjusts for changes in the solar panel's generation capacity and terminal voltage. This unit is determined based on the calculated PV power and PCC voltage.

$$I_{pvff} = \frac{2P_{pv}}{3V_t} \quad (4)$$

A proportional integral (PI) regulator takes the error among $V_{DC_{ref}}$ and VDC as input and generates the loss component (Iloss). The calculation of the loss component is as follows:

$$I_{loss} = \left(K_p + K_i / s\right)(V_{DCref} - V_{DC}) \quad (5)$$

2.3.4 Load Fundamental Current Magnitude Estimation

The organizational assembly of the ESOGI-FLL is depicted in Fig. 5, which consists of two key blocks: the modified SOGI and the frequency locked loop. The FLL controller employs the in-phase component (i_{id}) and the quadrature section (i_{lq}) of the load current to estimate the frequency of the grid. The transfer function for the input current i_L is shown as, where i_L has an amplitude of $i_{\alpha p}$ and a DC offset of 'A'.

$$I_L(s) = \frac{I_{ap\omega'}}{2} + \frac{A}{s} \quad (6)$$

$$I_{ld}(s) = \frac{k\omega' s}{s^2 + k\omega' s + \omega'^2} I_L(s) \quad (7)$$

$$L_{lq}(s) = I_{lq}(s) = \frac{ks^2}{s^2 + k\omega' s + \omega'^2} I_L(s) \quad (8)$$

$$I_{ld}(s) = \frac{k\omega' s}{s^2 + k\omega' s + \omega'^2} (I_{\alpha p} \frac{\omega'}{s^2 + \omega'^2} + \frac{A}{s}) \quad (9)$$

$$I_{ld}(s) = I_{\alpha p} \frac{\omega'}{s^2 + \omega'^2} + \frac{(kA - I_{\alpha p})}{s^2 + k\omega' s + \omega'^2} \quad (10)$$

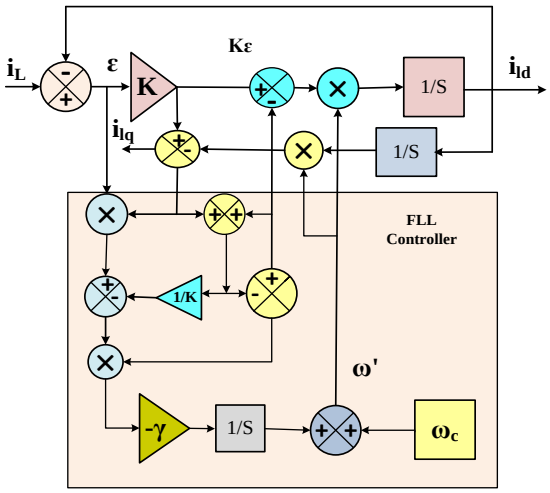

Fig.5. Load fundamental current magnitude estimation

The time response of the quadrature mechanisms and the in-phase of the generalized integrator is investigated by reflecting the DC section in the current of the load. Consequently, the quadrature mechanisms and the in-phase of the basic load are obtained. The quadrature and in-phase sections of the fundamental current are presented as follows:

$$I_{lq}(s) = \frac{ks^2}{s^2 + k\omega' s + \omega'^2} (I_{\alpha p} \frac{\omega'}{s^2 + \omega'^2} + \frac{A}{s}) \quad (11)$$

$$I_{lq}(s) = \frac{I_{\alpha p} s}{s^2 + \omega'^2} + \frac{(kA - I_{\alpha p})s}{s(s^2 + k\omega' s + \omega'^2)} \quad (12)$$

The time-domain representation of the fundamental load components (I_{ld}) and (I_{lq}) is obtained by converting them as follows:

$$i_{ld}(t) = I_{\alpha p} \sin(\omega' t) + \frac{(kA - I_{\alpha p})}{\sqrt{1 - \left(\frac{k}{2}\right)^2}} e^{\frac{-k\omega' t}{2}} \times \sin\left(\omega' t \sqrt{1 - \left(\frac{k}{2}\right)^2}\right) \quad (13)$$

$$i_{lq}(t) = I_{\alpha p} \cos(\omega' t) + \frac{(kA - I_{\alpha p})}{\sqrt{1 - \left(\frac{k}{2}\right)^2}} e^{\frac{-k\omega' t}{2}} + \cos^{-1}\left(\left(\frac{k}{2}\right)^2\right) \quad (14)$$

Fundamental load relations are determined from these i_{ld} and i_{lq} equations, as demonstrated in Fig. 5. In stable state conditions with DC offset, the performance of the regulator process is not affected by the in-phase vital component of the load. The quadrature section of the vital load current (i_{lq}) is orthogonal to the load current. To estimate the grid frequency for the FLL controller, the quadrature section of the vital current of the load (i_{lq}) and the error among the current of the load and the in-phase section (i_{ld}) are used. Additionally, the DC offset in the load component does not affect the performance of the FLL in steady-state operating conditions. As a result, the ESOGI-FLL's frequency-adaptive structure is reliable and effective for estimating the grid's frequency. By using unit templates, sample and hold logics, zero crossing detectors, and zero crossing detectors for the appropriate phases, the magnitude of the three fundamental load currents $((I_{\alpha p}, I_{bp}, I_{cp})$ are determined. The overall reference grid current weight is determined by considering the load, feed-forward, and loss components. The net load section (I_{load}) of the currents of load is calculated and used in combination with the other components to evaluate the overall weight of the grid reference current. Specifically, the evaluation of the reference grid current's weight is carried out as follows:

2.3.5 Estimation of Grid Current Reference

To produce the reference for the currents of grid $(i_{aref}, i_{bref}, i_{cref})$, the net load component is utilized by the corresponding unit templates (u_{pa}, u_{pb}, u_{pc}).These estimated values are then compared to the detected grid currents to create the current error, which is fed into the hysteresis current controller for generating the voltage source inverter switching pulses.

$$I_{load} = \frac{I_{ap} + I_{bp} + I_{cp}}{2} \quad (15)$$

$$I_{net} = -I_{load} + I_{pvff} - I_{loss} + I_{battery} \quad (16)$$

$$i_{aref} = u_{pa} \times I_{net} \quad (17)$$

$$i_{bref} = u_{pb} \times I_{net} \quad (18)$$

$$i_{cref} = u_{pc} \times I_{net} \quad (19)$$

3. Simulation Results

The Sim Power System Toolbox is used in MATLAB and Simulink to simulate an ESOGI-FLL-controlled PV Battery integrated grid system. The rating of PV is 725 volts & 95.92 kW, the rating of battery is 480 volts & 500 Ah, the RL value of the non-linear load is 120 Ω & 0.15 mH, and the system is a 400-volt, 50 Hz grid system. The functioning of the scheme is examined for variations in solar irradiation, load-side network unbalance, and non-linear load conditions. The system's response is illustrated through various signals such as PV voltage, PV current, PV power, battery voltage, battery current, battery power, battery state of charge, grid voltage, grid current, load current, inverter current, grid power, and DC link voltage.

3.1 Dynamic Performance of the PV Battery Integrated Grid System

Fig. 6 depicts the waveforms of several signals to illustrate the system response under unbalanced load conditions. Specifically, Fig. 6 (a) shows the PV voltage, current, and power waveforms, while Fig. 6 (b) displays the waveforms of battery voltage, current, and state of charge. The inverter voltage and current waveforms are shown in Fig. 6 (c), while Fig. 6 (d) shows the Load voltage and current waveforms. The waveforms of grid voltage and current are shown in Fig. 6 (e), and Fig. 6 (f) presents the waveforms of grid real and reactive power. The PV voltage is maintained at 750 volts, the PV current is maintained at 126.66 A, and the PV power is maintained at 95.1 kW. The battery voltage is maintained at 500 volts, the battery current is maintained at -50 A, and the charging power is maintained at 25 kW. The battery is in charging mode in these conditions while examine the state of charge of the battery. The Inverter voltage is maintained at 400 volts on the line, and the inverter current is 150 A peak at each phase and supplies the harmonic compensation current to the point of common coupling. The load voltage is maintained at 400 volts, and the line and phase is disconnected from 0.05 to 0.15 seconds to create unbalanced load conditions in the system. The grid voltage is maintained at 400 volts, on the line and the grid current is maintained at 120 A peak at each phase. The grid's real power is around 70 kW, and the grid's reactive power is zero. This indicates the grid operated at unity power factor and the PV battery inverter supplies the reactive power to the load always. Also, during unbalanced conditions, grid current nature is sinusoidal, total harmonic distortion is less than 5 %, and the IEEE standard is obeyed.

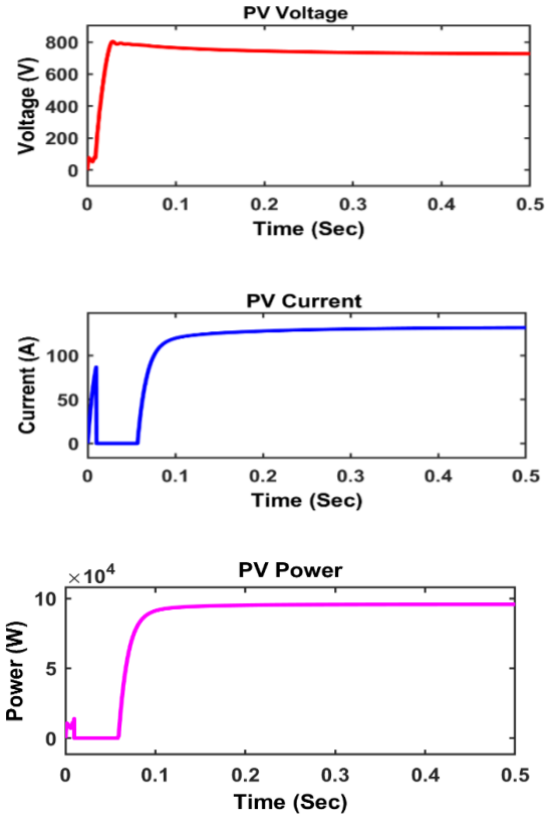

(a) PV Voltage, PV Current and PV Power

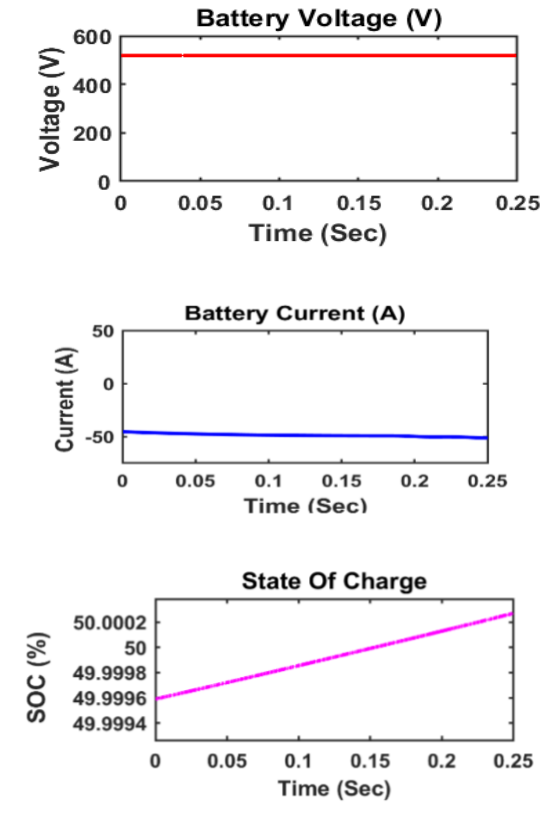

(b) Battery Voltage, Current and State of charge

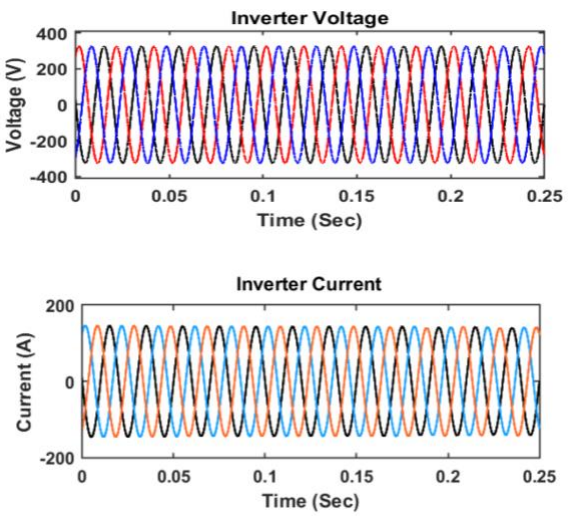

(c) Inverter Voltage and current

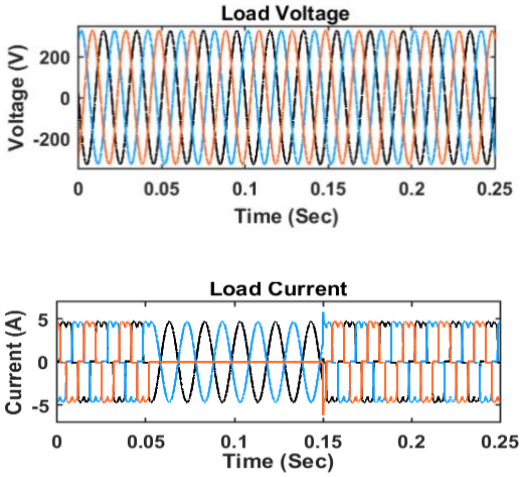

(d) Load Voltage and current

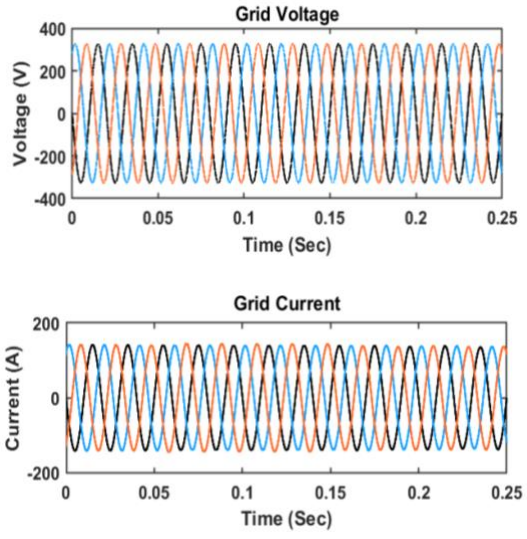

(e) Grid Voltage and Current

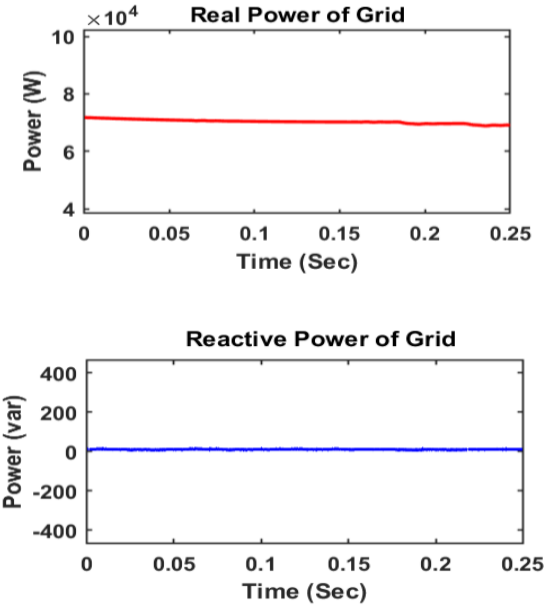

(f) Grid real power and reactive power

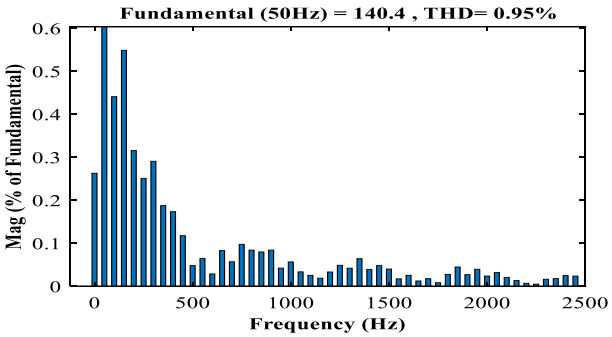

(g) Total Harmonic Distortion of grid current

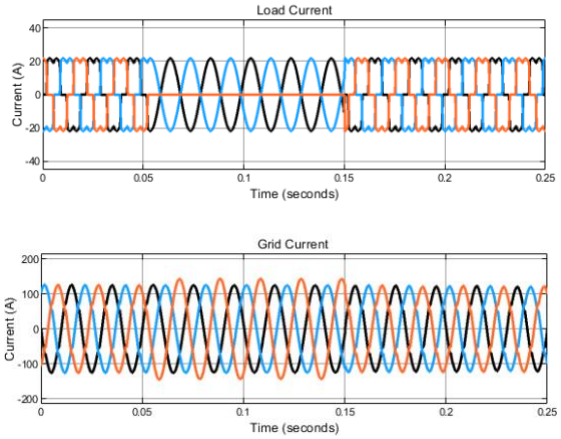

(h) Load and Grid current for increasing Load condition

Fig.6. Simulation result of PV battery integrated system with Unbalanced load conditions

3.2 Change Irradiance Conditions of the PV Battery Integrated Grid System

The voltage, current, and power waveforms of the PV system are illustrated in Fig. 7 (a), while Fig. 7 (b) displays the waveforms of battery voltage, current, and state of charge. The inverter voltage and current waveforms are shown in Fig. 7 (c), while Fig. 7 (d) demonstrates the load voltage and current waveforms. In Fig. 7 (e), the waveforms of grid voltage and current are displayed, while Fig. 7 (f) shows the grid's real and reactive power waveforms under changing irradiance conditions, first from 1000 W/m^2 to 500 W/m^2, and then back to 1000 W/m^2. The PV current and power change according to changing irradiance conditions. PV current is maintained at 66.66 A, and PV power is maintained at 50 kW at 500 W/m^2. The battery changes the mode from charging to discharging mode when the irradiance goes to 500 W/m^2 to supply power to the point of common coupling. The Inverter current and grid current change with changes in irradiance conditions. The load always getting supply form the system without any disturbance. The grid current's total harmonic distortion at 500 W/m^2 is 2.03 % only, and it obeys the IEEE power quality standards from Fig. 7 (g).

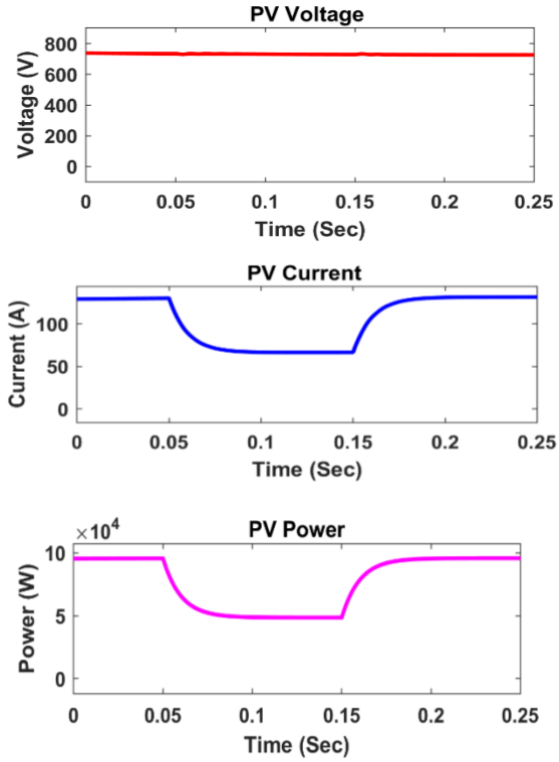

(a) PV Voltage, Current and Power

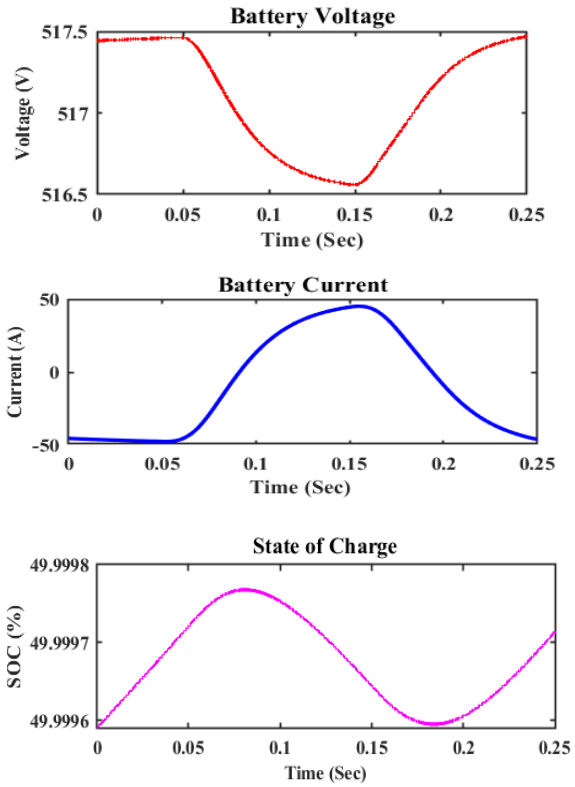

(b) Battery Voltage, Current and state of charge

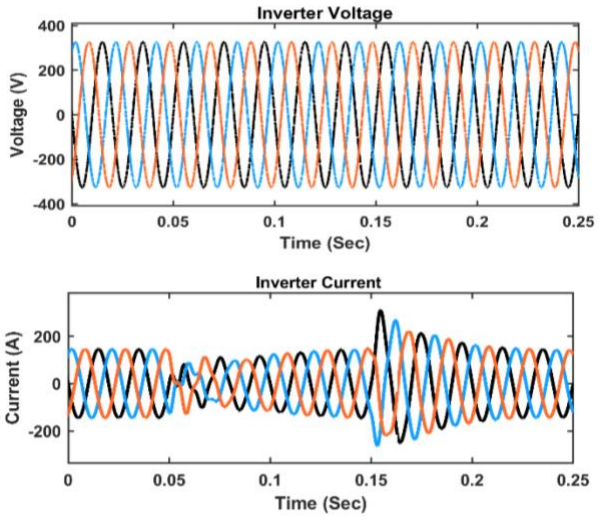

(c) Inverter Voltage and Current

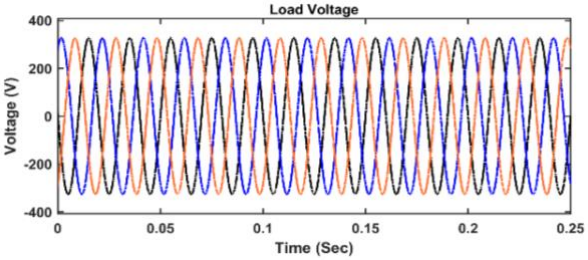

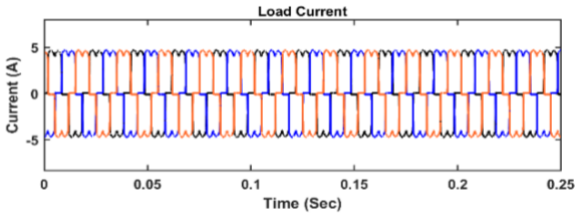

(d) Load Voltage and Current

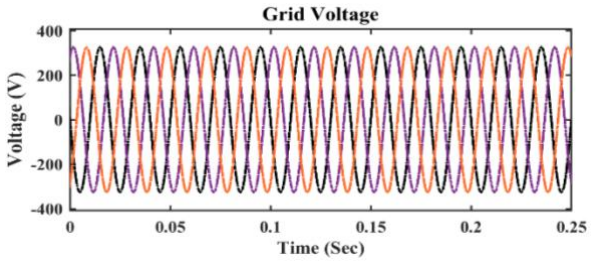

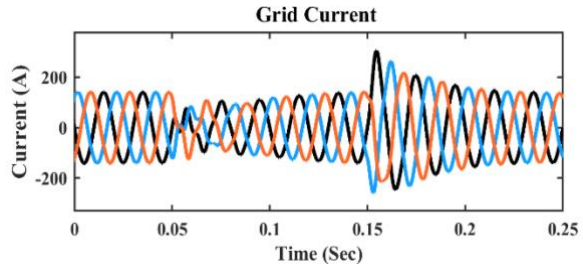

(e) Grid Voltage and Current

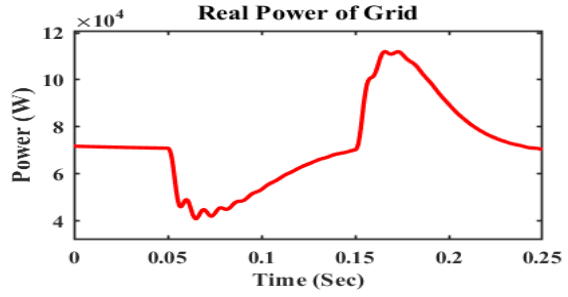

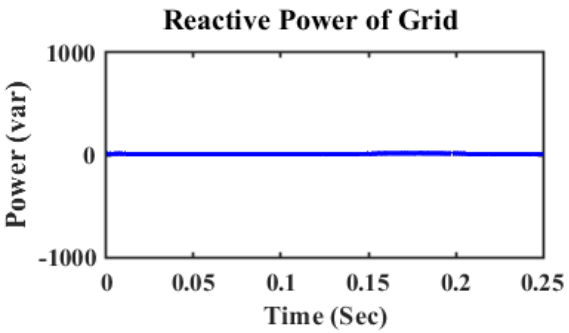

(f) Grid real and reactive power

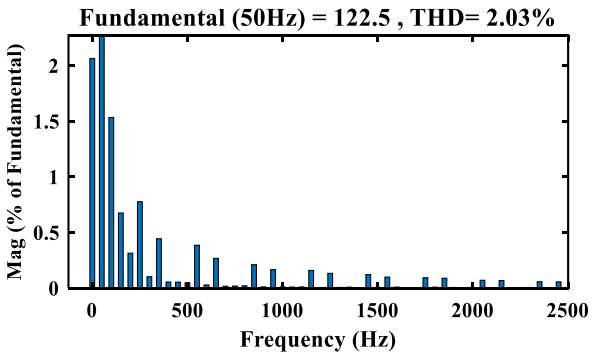

(g) Total Harmonic Distortion of the Current

Fig.7. Simulation result of PV battery integrated system with Change in irradiance conditions

4. Conclusion

To improve the quality of power in the delivery network, various techniques can be employed, including correction of the power factor, balancing of the load, and harmonic mitigation. These methods help in supplying the essential real power to the macro network while maintaining a high level of PQ in the proposed PV battery integrated grid system with an ESOGI-FLL-based controlling procedure. The peak power from the PV array was efficiently harvested using the PSO-ANFIS MPPT method, which also maintained the DC link voltage at the optimum level. By efficiently extracting the quadrature section of the vital current of the load, the use of the ESOGI-FLL-based structure has resulted in an enhancement in the precision of the control procedure for the demonstrated system. The grid current's total harmonic distortion (THD) has been found to be well within the acceptable limits specified by the IEEE-519 standard, i.e., 0.95 % for unbalanced load conditions and 2.03 % for change in irradiance conditions. This work can be used in the PV power sector. And also, soft computing-based ESOGI is considered a future scope of work.

Nomenclature:

PV	**Photovoltaic**
VSC	Voltage Source Converter
MPC	Model Predictive Control
PGSs	Power Generating Schemes
PLL	Phase Lock Loop
LS	Least Square
LMS	Least Mean Square
SOGI	Second Order Generalised Integrator
SOGI-	Second Order Generalised Integrator

Q	Quadrature
PSO	Particle Swarm Optimisation
ANFIS	Adaptive Fuzzy Neuro Interface Systems
MPP	Maximum Power point
ESOGI	Enhanced Second Order Generalised Integrator
FLL	Frequency Lock Loop
G	Irradiation
T	Temperature
PQ	Power Quality
MPPT	Maximum Power Tracking
GMPP	Global Maximum Power point

References

[1] N. Kumar, B. Singh, and B. K. Panigrahi, "Integration of Solar PV Generation with Distribution Grid: Using Novel Adaptive Filter Based Control Technique," 2018 4th Int. Conf. Univers. Village, pp. 1–6, 2018.

[2] D. S. Shugar and S. Ramon, "Photovoltaic in the utility distribution system: the evaluation of system and distributed benefits," in Proc. IEEE Photovoltaic Specialist Conference, pp. 836-843, 21-25 May, 1990.

[3] A. Gupta, P. Kumar, Rupendra K. Pachauri, Y. K. Chauhan, "Effect of Environmental Conditions on Single and Double Diode PV System: A Comparative Study", International Journal of Renewable Energy and Research, vol. 4(4), 849-858, 2014.

[4] Xiao, F., Dong, L., Li, L., & Liao, X. (2017). A Frequency-Fixed SOGI-Based PLL for Single-Phase Grid-Connected Converters. IEEE Transactions on Power Electronics, 32(3), 1713–1719. https://doi.org/10.1109/TPEL.2016.2606623

[5] T. F. Wu, C. H. Chang, L. C. Lin and C. L. Kuo, "Power loss comparison of single- and two-stage grid-connected photovoltaic systems," IEEE Transactions Energy Conversion, vol. 26, no. 2, pp. 707-715, 2011.

[6] A. S. O. Ogunjuyigbe, T. R. Ayodele, V. E. Idika and O. Ojo, "Effect of lamp technologies on the power quality of electrical distribution network," in Proc. IEEE Power Energy System, pp. 159-163, 2017.

[7] X. Liang, "Emerging power quality challenges due to integration of renewable energy sources," IEEE Transactions Industry Applications, vol. 53, no. 2, pp. 855-866, 2017.

[8] A. Javadi, A. Hamadi and K. Al-Haddad, "Three-phase power quality device tor weak Systems based on SRF and p-q theory controller," in Proc. IEEE Industrial Electronics Society, pp. 345-350, 2015.

[9] R. K. Agarwal, I. Hussain and B. Singh, "LMF-based control algorithm for single stage three-phase grid integrated solar PV system," IEEE Transactions Sustainable Energy, vol. 7, no. 4, pp. 1379-1387, 8d585+.2016.

[10] L. Tarisciotti, "Model predictive control for shunt active filters with fixed switching frequency," IEEE Transactions Industry Applications, vol. 53, no. 1, pp. 296-304, 2017.

[11] B. Singh, C. Jain, S. Goel, A. Chandra and K. Al-Haddad, "A multifunctional grid-tied solar energy conversion system with ANF-based control approach," IEEE Transactions Industry Applications, vol. 52(5), pp. 3663-3672, 2016.

[12] S. W. Kang and K. H. Kim, "Sliding mode harmonic compensation strategy for power quality improvement of a grid-connected inverter under distorted grid condition," IET Power Electronics, vol. 8, no. 8, pp. 1461- 1472, 2015.

[13] R. Panigrahi and B. Subudhi, "Performance enhancement of shunt active power filter using a Kalman filter-based H-infinity control strategy," IEEE Transactions Power Electronics, vol. 32, no. 4, pp. 2622-2630, 2017.

[14] I. Kamwa and R. Grondin, "Fast adaptive schemes for tracking voltage phasor and local frequency in power transmission and distribution systems," IEEE Transactions Power Delivery, vol. 7, no. 2, pp. 789-795, 1992.

[15] Y. Abdelkader, T. Allaoui, C. Abdelkader, "Power Quality Improvement Based on Five-Level Shunt APF Using Sliding Mode Control Scheme Connected to a Photovoltaic. International Journal of Smart Grid", vol. 1(1), pp. 1-14, 2017.

[16] D. S. Ochs, B. Mirafzal and P. Sotoodeh, "A method of seamless transitions between grid-tied and stand-alone modes of operation for utility-interactive three-phase inverters," IEEE Transactions Industry Applications, vol. 50, no. 3, pp. 1934-1941, 2014.

[17] N. Sung, J. Lee, B. Kim, M. Park, and I.-K. Yu, "Novel concept of a PV power generation system adding the function of shunt active filter," in Proc. IEEE/PES Trans. Distrib. Conf. Exhib, vol. 3, pp. 1658–1663, 2002.

[18] B. Singh, P. Jayaprakash, S. Kumar and D. P. Kothari, "Implementation of neural-network-controlled three-leg VSC and a transformer as three-phase four-wire DSTATCOM," IEEE Transactions Industry Applications, vol. 47, no. 4, pp. 1892-1901, 2011.

[19] M. Qasim and V. Khadkikar, "Application of artificial neural networks for shunt active power filter control," IEEE Transactions Industrial Informatics, vol. 10, no. 3, pp. 1765-1774, 2014.

[20] T. Penthia, A. K. Panda, S. K. Sarangi and M. Mangaraj, "ADALINE based LMS algorithm in a three phase four wire distribution system for power quality enhancement," in Proc. IEEE 6th

International Conference on Power Systems (ICPS), pp. 1-5, 2016.
[21] P. Shah, I. Hussain and B. Singh, "Real-time implementation of optimal operation of single-stage grid interfaced PV system under weak grid conditions" IET Generation Transmission and Distribution, Early Access.
[22] A. Adib, B. Mirafzal, X. Wang and F. Blaabjerg, "On stability of voltage source inverters in weak grids," IEEE Access, vol. 6, pp. 4427-4439, 2018.
[23] S. Kumar, I. Hussain, B. Singh, A. Chandra and K. Al Haddad, "An adaptive control scheme of SPV system integrated to three phase AC distribution system," IEEE Transactions Industry Applications, vol. 53, no. 6, pp. 5173-5181, 2017.
[24] C. Jain and B. Singh, "A SOGI-FLL based control algorithm for single phase grid interfaced multifunctional SPV under non ideal distribution system," in Proc. IEEE India Conference (INDICON), Pune, pp. 1-6, 2014.
[25] P. Shah. I. Hussain and B. Singh, "Single stage SECS interfaced with grid using ISOGI-FLL based control algorithm" in Proc. IEEE India International Conf. Power Electronics (IICPE), pp. 1-6, 2016.
[26] P. Shah, I. Hussain and B. Singh, "Multi-resonant FLL based control algorithm for grid interfaced multi-functional solar energy conversion" IET Science, Measurement & Technology, vol. 12, no. 1, pp. 49-62, 2018.
[27] A. Luo, Y. Chen, Z. Shuai and C. Tu, "An improved reactive current detection and power control method for single-phase photovoltaic grid connected DG system," IEEE Transactions Energy Conversion, vol. 28, no. 4, pp. 823-831, Dec. 2013.
[28] B. Singh, A. Chandra and K. Al-Haddad, Power quality: problems and mitigation techniques, John Wiley & Sons Ltd., United Kingdom, 2015.
[29] Ho Soonmin, Masoud Taghavi, "Solar Energy Development: Study Cases in Iran and Malaysia," International Journal of Engineering Trends and Technology, vol. 70, no. 8, pp. 408-422, 2022.
[30] F. K. Alhousni, F. B. Ismail, P. C. Okonkwo, H. Mohamed, B. O. Okonkwo, O. A. Al-Shahri, "A Review of PV solar energy system operations and applications in Dhofar Oman", AIMS Energy, vol. 10(4), pp. 858-884, 2022.
[31] Golestan, S., Guerrero, J. M., Vasquez, J. C., Abusorrah, A. M., & Al-Turki, Y. (2019). Single-Phase FLLs Based on Linear Kalman Filter, Limit-Cycle Oscillator, and Complex Bandpass Filter: Analysis and Comparison with a Standard FLL in Grid Applications. IEEE Transactions on Power Electronics, 34(12), 11774–11790. https://doi.org/10.1109/TPEL.2019.2906031
[32] Xin, Z., Wang, X., Qin, Z., Lu, M., Loh, P. C., & Blaabjerg, F. (2016). An Improved Second-Order Generalized Integrator Based Quadrature Signal Generator. IEEE Transactions on Power Electronics, 31(12), 8068–8073. https://doi.org/10.1109/TPEL.2016.2576644
[33] Abdelkader, Y., Allaoui, T., & Abdelkader, C. (2017). Power Quality Improvement Based on Five-Level Shunt APF Using Sliding Mode Control Scheme Connected to a Photovoltaic. International Journal of Smart Grid, 1(1). https://doi.org/10.20508/ijsmartgrid.v1i1.4.g4
[34] Belkaid, A., Colak, I., Kayisli, K., & Bayindir, R. (2020). Improving PV System Performance using High Efficiency Fuzzy Logic Control. 8th International Conference on Smart Grid, IcSmart Grid 2020, V, 152–156. https://doi.org/10.1109/icSmartGrid49881.2020.9144817